RESEARCH ARTICLE

Proceedings of the 39th Informal Meeting on Mass Spectrometry

Estimation of thermodynamic and physicochemical properties of the alkali astatides: On the bond strength of molecular astatine (At$_2$) and the hydration enthalpy of astatide (At$^-$)

Peter C. Burgers[1] (ORCID) | Lona Zeneyedpour[1] | Theo M. Luider[1] | John L. Holmes[2]

[1]Department of Neurology, Laboratory of Neuro-Oncology, Erasmus Medical Center, Rotterdam, The Netherlands

[2]Department of Chemistry and Biological Sciences, University of Ottawa, Ottawa, Canada

Correspondence
Peter C. Burgers, Department of Neurology, Laboratory of Neuro-Oncology, Erasmus Medical Center, Rotterdam, 3015 CN, The Netherlands.
Email: p.burgers@erasmusmc.nl

Abstract

The recent accurate and precise determination of the electron affinity (*EA*) of the astatine atom At^0 warrants a re-investigation of the estimated thermodynamic properties of At^0 and astatine containing molecules as this *EA* was found to be much lower (by 0.4 eV) than previous estimated values. In this contribution we estimate, from available data sources, the following thermodynamic and physicochemical properties of the alkali astatides (MAt, M = Li, Na, K, Rb, Cs): their solid and gaseous heats of formation, lattice and gas-phase binding enthalpies, sublimation energies and melting temperatures. Gas-phase charge-transfer dissociation energies for the alkali astatides (the energy requirement for M$^+$At$^- \rightarrow$ M^0 + At^0) have been obtained and are compared with those for the other alkali halides. Use of Born-Haber cycles together with the new *AE* (At^0) value allows the re-evaluation of ΔH_f (At^0)$_g$ (=56 ± 5 kJ/mol); it is concluded that (At$_2$)$_g$ is a weakly bonded species (bond strength <50 kJ/mol), significantly weaker bonded than previously estimated (116 kJ/mol) and much weaker bonded than I$_2$ (148 kJ/mol), but in agreement with the finding from theory that spin-orbit coupling considerably reduces the bond strength in At$_2$. The hydration enthalpy (ΔH_{aq}) of At$^-$ is estimated to be −230 ± 2 kJ/mol (using ΔH_{aq}[H$^+$] = −1150.1 kJ/mol), in good agreement with molecular dynamics calculations. Arguments are presented that the largest alkali halide, CsAt, like the smallest, LiF, will be only sparingly soluble in water, following the generalization from hard/soft acid/base principles that "small likes small" and "large likes large."

KEYWORDS
alkali astatides, astatine, Born-Haber cycle, solubilities, thermodynamic properties

1 | INTRODUCTION

Astatine or element 85 occurs on earth with an estimated total abundance of less than 1 g.[1] One of its longest-lived isotopes, ^{211}At with a half-life of 7.2 h, is of considerable interest as an α particle emitting radionuclide for targeted alpha therapy (TAT),[2–4] but only nanogram quantities are available through synthetic methods.[5–8] ^{211}At can be produced by bombarding natural bismuth metal targets with α-particles, but the beam energy should be carefully controlled to avoid formation of ^{210}At, which decays to the extremely toxic ^{210}Po. Recently,

sodium astatide, $Na^{211}At$, was produced and successfully used as a therapeutic drug, leading to marked tumor regression effects in mice that had received grafts of thyroid cancer cells.[9,10] Thus, there is renewed interest in the properties of astatine and astatine containing compounds as exemplified by the recent formation of the World Astatine Community (WAC). One of the properties that has received considerable attention over recent years is the electron affinity (*EA*) of At^0, that is, the energy gain for the process $At^0 + e^- \rightarrow At^-$. The *EA* of an element is an important property as it determines its electronegativity ($EN = \frac{1}{2}\{IE + EA\}$, Mulliken scale, where *IE* is the ionization energy) and electrophilicity ($\omega = \frac{1}{4}\{IE + EA\}^2/\{IE - EA\}$). Earlier estimates of *EA* (At^0) are all 2.8 eV (270 kJ/mol)[11] and already in 1969 Zollweg[12] proposed the value 2.8 ± 0.2 eV. In fact, a happy state of affairs existed where all estimated thermodynamic values of At^0 were reasonably consistent,[11] for example $\Delta H_f (At^0)_g = 92$ or 97 kJ/mol, $\Delta H_f (At^-)_g = -197, -191$ or -179 kJ/mol with an *EA* of about 270 kJ/mol. However, various recent ab initio calculations[13–17] predicted a much smaller value, for example *EA* (At^0) = 2.423 ± 0.013 eV.[13] The *EA* of At^0 was recently measured by Leimbach et al.,[18] *EA* (At^0) = 2.41578 ± 0.00007 eV, and thus the calculations are in excellent agreement with experiment. The implications for the smaller *EA* on other properties derived from *EA* and *IE* (such as *EN*, ω, hardness and softness) have been addressed by Leimbach et al; thus, for example the molecule HAt is better described as the hydride, AtH. The *EA* measurement of Leimbach et al has important consequences for other aspects of astatine chemistry, such as the dissociation energy of At_2 and for curve crossing in the dissociation of the alkali astatides, on which we report here. For example, for At_2, if the above

$\Delta H_f (At^-)_g$ values are correct, then from the measured *EA* (At^0) and the estimated $\Delta H_f (At_2)_g = 84 \pm 11$ kJ/mol,[19] a dissociation energy for At_2 of -12 to $+24$ kJ/mol is calculated, significantly below the estimated value of 116 kJ/mol[20] (or even negative).

Thermodynamic properties of astatine containing molecules have been estimated using various inter- and extrapolation procedures.[11] We consider here the alkali astatides from which earlier estimates of *EA* (At^0) originate. A representative energy diagram (Born Haber cycle) of the alkali halides (MX) is presented in Figure 1, which shows the relationships between various thermodynamic properties. The Figure is scaled to represent NaCl. It can be seen that for the alkali halides, the following equations hold:

$$\Delta H_f (MX)_g = \Delta H_f (M^+)_g + \Delta H_f (X^-)_g - GBE \quad (1)$$

$$\Delta H_f (MX)_s = \Delta H_f (M^+)_g + \Delta H_f (X^-)_g - LBE \quad (2)$$

where MX is the alkali halide, ΔH_f represents the heat of formation at 298 K, g and s represent values for gas-phase and solid species respectively, and *GBE* and *LBE* are the gas-phase and lattice binding enthalpies respectively. These binding energies are relative to M^+ and X^-, ("heat of ionic dissociation")[21,22]; the gas-phase *dissociation* energy (*D*) shown in Figure 1 is relative to neutral Na^0 and Cl^0 and is the result of charge transfer. Note that for all alkali halides these dissociation energies $MX \rightarrow M^0 + X^0$ are smaller than their binding energies, $MX \rightarrow M^+ + X^-$. In the present paper, we have collected from various sources the thermodynamic properties of the solid and
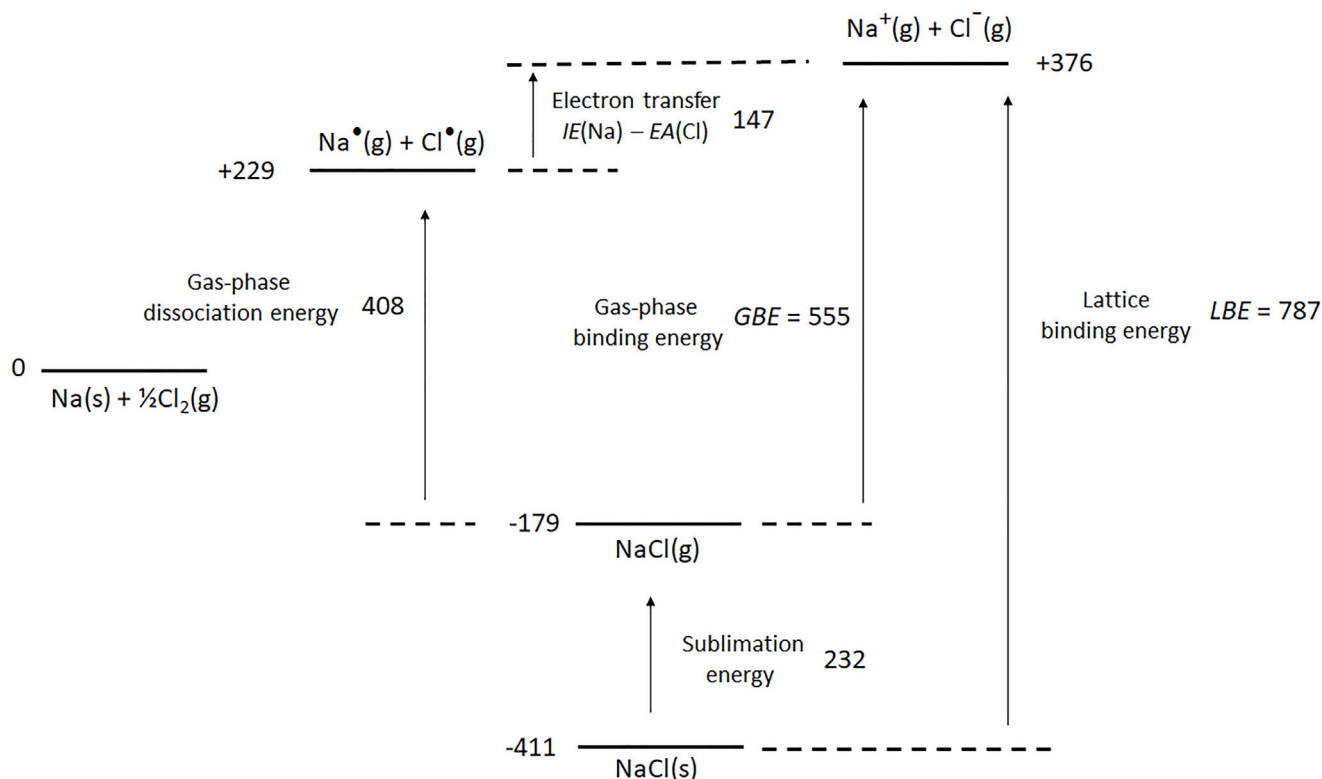

FIGURE 1 Energy diagram (Born Haber cycle) for NaCl. Values in kJ/mol.

gaseous alkali halides. It has been reported previously[23] that the inter-ionic distance in $(MX)_s$ is a good parameter for relevant thermody-namic properties of $(MX)_s$ such as their heats of formation, lattice binding enthalpies and sublimation enthalpies. We have extended this finding to gas-phase species and have used this approach to (re-)esti-mate various thermodynamic properties of the alkali astatides, from which $\Delta H_f (At^-)_g$ is derived using Equations (1) and (2). From the mea-sured EA, $\Delta H_f (At^0)_g$ is obtained and from the previously estimated $\Delta H_f (At_2)_g$, the bond strength of the dihalogen At_2 can be assessed.

2 | RESULTS AND DISCUSSION

2.1 | Reference data for solid-phase alkali halides

The bond lengths of $(MX)_s$ were taken from Sirdeshmukh et al,[24] see Table 1. The relevant heats of formation (298 K) of $(MX)_s$ are available from the NIST-JANAF tables[25] and from the NBS database[26] Where they overlap, agreement is good. These data are collected in Table 1.

Lattice binding energies (*LBE*) can be found in various (review) papers, for example, by Kaya,[27] Morris[28] and Woodcock,[29] see Table 1.[30] Agreement between the different data sources is in general quite good. The *LBE*'s reported by Kaya are the recommended values determined by the Born–Fajans–Haber (BFH) cycle,[27] and we have used these values (column [d]) in the present study. These *LBE* values

are also in best agreement with those calculated from Equation (2) using the ΔH_f values of column (c) (deviation 6 ± 5 kJ/mol, with the largest deviation for CsF, 17 kJ/mol; these matters deserve further evaluation, but do not change our conclusions).

It had been emphasized by several authors that the trend in lat-tice binding energy is very regular among the alkali halides.[23,31,32] As can be seen from Figure 2, the *LBE*'s show an inverse proportionality with d (*LBE* = 1810.8/d + 142.29 [R^2 = 0.9972]), which reproduces *LBE* to an average of 6 kJ/mol (with maximum deviations of +12 kJ/mol for LiI, −9 kJ/mol for KBr and +9 kJ/mol for CsCl, experimental minus calculated values) but note that this line does not go through the origin. The *LBE*'s can be calculated from the Born–Landé equation, also linear in 1/d: $LBE = [1,389*M*(1–1/n)]/d$ where M is the Made-lung constant, n is the Born exponent[33] and 1,389 is the Coulomb constant (in (kJ/mol)*Å*e^{-2}). For example, for NaCl, an *LBE* of 766 is thus calculated compare Table 1 (M (NaCl) = 1.748, n (NaCl) = 9.1 from compressibility data[33]).

Oshchapovskii[34,35] has derived an equation for the *LBE*'s for the alkali halides:

$$LBE\,(kJ/mol) = C\{(1-a)/(R-b)\} \tag{3}$$

where C is a proportionality constant (to be determined from the database used), $R = R_1 + R_2$, $a = R_1 R_2 / d^2$, $b = (\pi/4)(R_1 R_2 / d)^2$, R_1 and R_2 are the crystal ionic radii for 6-coordination in Å for the metal

TABLE 1 Bond lengths (d, Å), heats of formation ($\Delta H_f (MX)_s$), lattice binding energies (*LBE*) of solid alkali halides MX and sum of hydration enthalpies of M^+ and X^- ($-\Sigma\Delta H_{aq}$).

MX	d	$\Delta H_f (MX)_s$			LBE			$-\Sigma\Delta H_{aq}$
	(a)	(b)	(c)		(d)	(e)	(f)	(g)
LiF	2.0131	−616.9	−616.0		1,036	1,021	1,040	1,042
LiCl	2.5699	−408.3	−408.6		853	841	858	898
LiBr	2.7508	−350.9	−351.2		807	808	822	867
LiI	3.0060	−270.0	−270.4		757	753	766	825
NaF	2.3164	−575.4	−576.6		923	908	923	927
NaCl	2.8200	−411.1	−411.2		786	774	804	783
NaBr	2.9865	−361.4	−361.1		747	745	754	752
NaI	3.2364	−287.9	−287.8		704	699	705	710
KF	2.6720	−568.6	−567.3		821	816	820	844
KCl	3.1464	−436.7	−436.6		715	715	719	700
KBr	3.2991	−393.8	−393.8		682	690	691	669
KI	3.5327	−327.9	−327.9		649	653	650	627
RbF	2.8258		−557.7		785	774	785	819
RbCl	3.2949		−435.4		689	678	692	675
RbBr	3.4454		−394.6		660	657	666	644
RbI	3.6710		−333.8		630	623	629	602
CsF	3.0100	−554.7	−553.5		740	724	733	794
CsCl	3.568	−442.3	−443.0		659	649	676	650
CsBr	3.7198		−405.8		631	632	653	619
CsI	3.9548		−346.6		604	598	618	577

Note: All values in kJ/mol. (a) Sirdeshmukh et al.[24] (b) NIST.[25] (c) Wagman et al.[26] (d) Kaya and Kaya.[27] (e) Morris.[28] (f) Woodcock.[29] (g) Housecroft and Jenkins.[30]
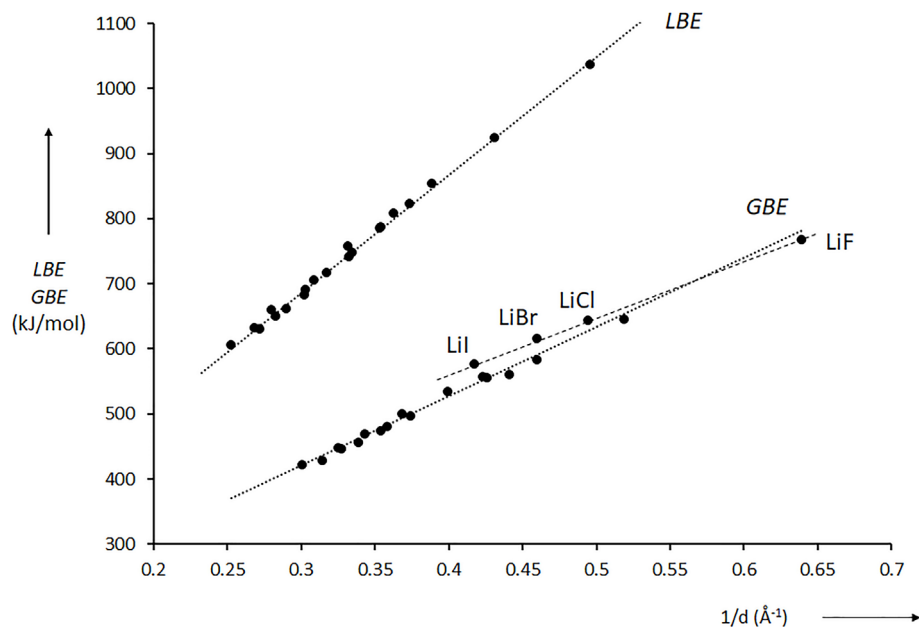
FIGURE 2 Lattice binding energies (*LBE*, kJ/mol) and gas-phase binding energies (*GBE*, kJ/mol) of the alkali halides as function of reciprocal bond length 1/d ($Å^{-1}$).

cation and halogen anion. From the *LBE* data in column (d) of Table 1, we obtain C = 2,533 ± 17 (ionic radii from Liu and Li[36]). This equation works very well, the *LBE*'s thus calculated are accurate to within 5 kJ/mol. For example, for NaCl an *LBE* of 784 kJ/mol is calculated by Equation (3), very close to the experimental value of 786 kJ/mol. Other empirical equations proposed to calculate *LBE*'s include the absolute hardness of the cations and anions.[37] A very accurate method for estimating *LBE*'s involves a graph of atomic orbitals (GAO) approach using quantitative structure–property relationships (QSPR), but this was not performed for the alkali astatides.[38] Using this approach the *LBE* of NaCl was calculated with an impressive accuracy of 0.3 kJ/mol as 785.7 kJ/mol.

It has been observed by several authors that the trends in heats of formation of the alkali halides are not as regular as the trends in lattice energies.[23,32] However, and as noted by Nasar,[23] for the subfamilies containing a common metal cation, very good linear correlations are observed, with R^2 exceeding 0.999. This is shown in Figure 3B for the solid alkali halides. Thus, the ΔH_f (MX)$_s$ data are divided into five subfamilies, each having four members containing a common metal ion. It can be seen that for a common cation, ΔH_f (MX)$_s$ becomes less negative, that is to say (MX)$_s$ becomes less stable with respect to (M)$_s$ and ½(X$_2$)$_g$ (X = F, Cl) or ½(X$_2$)$_l$ (X = Br) or ½(X$_2$)$_s$ (X = I) as d increases. However, for a common halide anion an opposite, non-linear and much smaller trend with d is observed and thus only the size of the halide anion plays a decisive role in the heats of formation of the alkali halides, as was discussed in an earlier paper.[23] The linear relationships observed in Figure 3B, where the metal ion is kept constant, may be exploited for estimation purposes of the heats of formation of the solid alkali astatides, provided their bond lengths can be assessed, as discussed below.

Similar observations pertain to gaseous alkali halides, see Figure 2 (plot of *GBE* against 1/d for *all* gaseous alkali halides) and Figure 3A (plots of ΔH_f (MX)$_g$ versus d for the subfamilies having a common metal ion), which are discussed in the next section.

2.2 | Reference data for gas-phase alkali halides

The bond lengths d of (MX)$_g$ were taken from Hargittai[39] and are known to a high degree of accuracy and precision. We have used the spectroscopic style for the precisions,[40] see Table 1, column (a).

The relevant heats of formation of (MX)$_g$ in Table 1 are available from the NIST-JANAF tables[25] and NBS database[26] as well as from the GIANT Tables.[41] Available error bars are also given. Dissociation energies D_o from which ΔH_f (MX)$_g$ may be calculated, can also be found in the Herzberg Tables[42] and in the original Brewer and Brackett compilation.[43] Accurate dissociation energies D_o have also been obtained by Su and Riley[44–46] and by Van Veen et al.[47] using photofragment spectroscopy from which ΔH_f (MX)$_g$ follows. The values of ΔH_f (MX)$_g$ are compiled in Table 2 and the agreement is usually good (within a few kJ/mol), except for CsF where relatively large differences ensue (up to 20 kJ/mol). The agreement between the Herzberg and Brewer and Brackett values (columns (g) and (h)) is striking and we have used the average of these values in our analyses. The measurements of Brewer and Brackett[43] are also in good agreement with theory.[48] We stress that our conclusions do not change when the other (slightly different) values are used.

For the gaseous species, plots of the heats of formation versus d were similar to those of the solid species; thus, linear relationships are obtained when the cation is kept constant, see Figure 3A, compare the corresponding plot for the solid alkali halides in Figure 3B.

The gas-phase binding energies, *GBE* (energy required for the process (MX)$_g$ → (M$^+$)$_g$ + (X$^-$)$_g$ can be calculated from Equation (1) using known heats of formation of gaseous M$^+$ and X$^-$ and these values are listed as the final entry in Table 2. A plot of *GBE* vs d (Figure 2) shows a linear relationship but not as good as *LBE* vs d, see also Figure 2. Notably, the gaseous lithium halides deviate from the line that unites
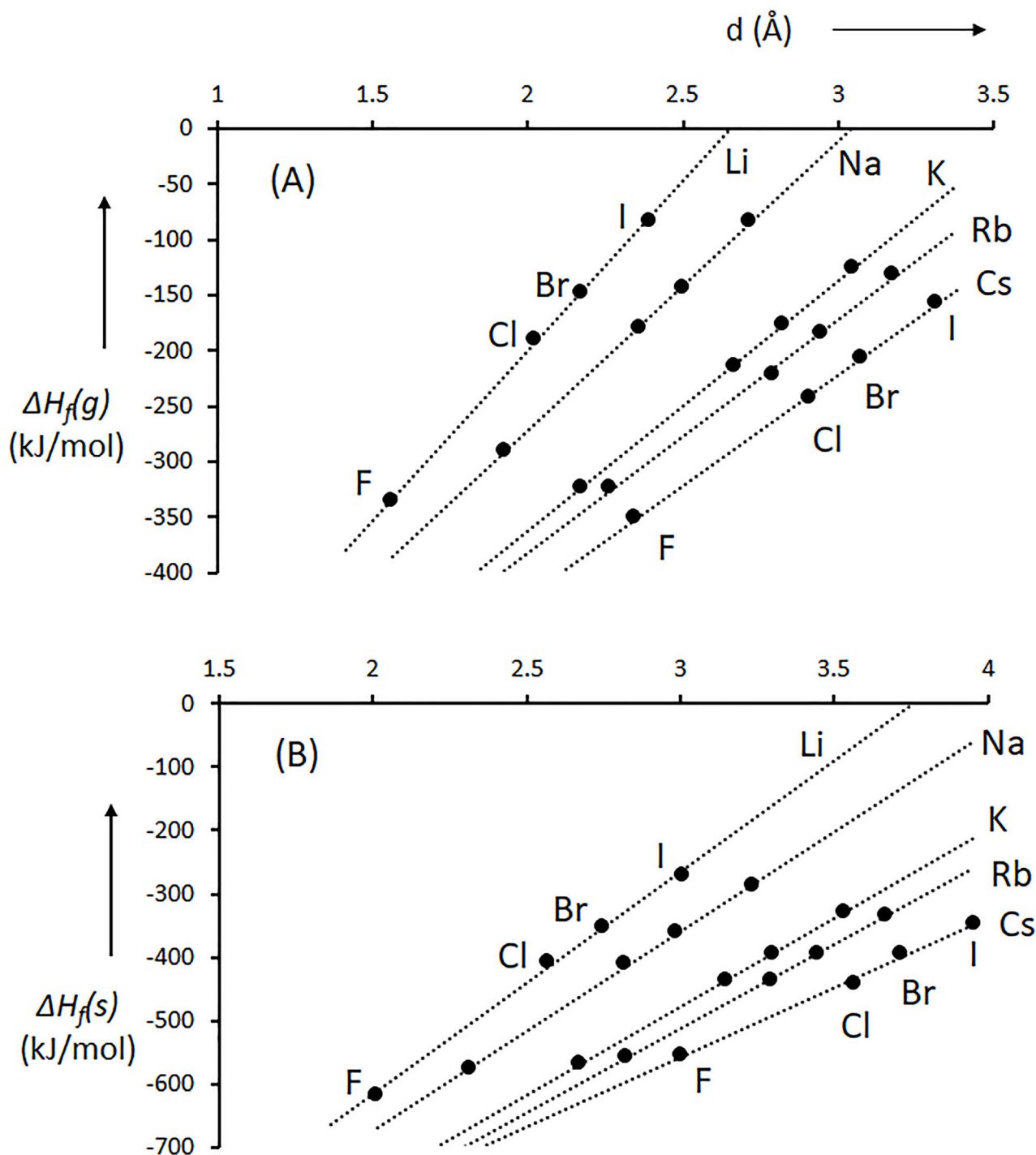
FIGURE 3 (A) Heats of formation of gaseous ($\Delta H_f(g)$, kJ/mol) and (B) solid ($\Delta H_f(s)$, kJ/mol) alkali halides as a function of bond length d (Å). Straight lines drawn for the subfamilies of common metal ions.

the others, whereas the solid lithium halides follow the general trend more closely.

It was found that good correlations for *GBE* and *LBE* are obtained for subfamilies containing a common metal ion, paralleling results for the heats of formation data, see above. We note that good correlations in subfamilies with a common metal ion have also observed for the melting temperatures,[35] see later.

2.3 | Estimation thermodynamic properties of the alkali astatides MAt and At$_2$

Figures 2 and 3 form the basis of the astatide estimations. *GBE* and *LBE* follow the equation

$$GBE\,(LBE) = \alpha/d + \beta \qquad (4)$$

and ΔH_f (g) and ΔH_f (s) follow

$$\Delta H_f = \gamma d - \delta \qquad (5)$$

where d is the alkali halide bond length (Tables 1 and 2) and α, β, γ and δ are empirical constants, which are given in Tables S1 and S2 together with R^2; correlations are generally very good.

We now need to assess the internuclear distances, d, of the alkali astatides (MAt) from which the various thermodynamic functions follow using the above equations and empirical parameters in Tables S1

and S2. For gaseous alkali astatides, d has been evaluated from DFT calculations[36] (table S1 from Liu and Li[36]), and these values are listed in Table 3. (It should be noted that these d values were derived from *scalar* relativistic calculations (i.e., without spin-orbit coupling, SOC, as opposed to 2 component (2c) and 4 component (4c) treatments, which include SOC) and so the computed distances for the alkali astatides may be somewhat too short.[49] These matters deserve further study; thus, it would be of interest to calculate d for gaseous MAt including SOC.)

The d values for solid MAt were derived from the linear relationships of internuclear distances d of solid and gaseous MX, for

TABLE 2 Bond lengths d (Å), heats of formation (ΔH_f (MX)$_g$), and binding energies (*GBE*) of gaseous alkali halides MX.

	d			$\Delta H_{f,}$(MX)g						*GBE*
	(a)	(b)	(c)	(d)	(e)	(f)	(g)	(h)	(i)
LiF	1.56389(5)	−340.8				−340	−331	−336	765
LiCl	2.02067(6)	−195.7	−196 ± 13			−195	−186	−187	640
LiBr	2.17042(4)	−154.0	−154 ± 13	−144 ± 4			−147	−148	615
LiI	2.39191(4)	−91.0	−91.0 ± 8.4	−75 ± 4		−81	−76	−88	574
NaF	1.92593(6)	−290.5				−291	−291	−290	645
NaCl	2.3606(1)	−181.4	−181 ± 2	−180 ± 8		−177	−179	−179	555
NaBr	2.50201(4)	−143.9	−143	−140 ± 4	−145 ± 1(2)	−143	−142	−144	533
NaI	2.71143(4)		−78	−86 ± 2	−93 ± 1(2)	−80	−75	−90	498
KF	2.17144(5)	−326.8				−325	−321	−322	581
KCl	2.6666(1)	−214.7	−214.7 ± 0.4	−219 ± 8		−214	−209	−214	493
KBr	2.82075(5)	−180.0	−180	−174 ± 4	−175 ± 1(2)	−180	−176	−179	473
KI	3.04781(5)	−125.5	−125.5 ± 2.1	−123 ± 2	−126 ± 1(2)	−126	−123	−125	444
RbF	2.26554(5)					−331	−322	−326	559
RbCl	2.78670(6)		−229	−222 ± 8		−229	−217	−219	475
RbBr	2.94471(5)		−183	−184 ± 4		−183	−183	−185	455
RbI	3.17684(5)		−133	−127 ± 2		−134	−131	−133	428
CsF	2.3453(1)	−356.5	−361			−359	−341	−344	547
CsCl	2.9062(1)	−240.2	−247	−240 ± 8		−240	−244	−246	470
CsBr	3.07221(5)		−200	−197 ± 4		−209	−214	−216	454
CsI	3.31515(6)		−154	−150 ± 2		−152	−160	−162	425

Note: Values in kJ/mol. (a) Hargittai[39] - precisions in spectroscopic style. (b) NIST.[25] (c) Lias et al.[41] (d) Previous works.[44–46] (e) van Veen et al.[47] (f) Wagman et al.[26] (g) Huber and Herzberg.[42] (h) Brewer and Brackett.[43] (i) Calculated from (h), using Equation (1); see text.

TABLE 3 Estimated thermodynamic properties (kJ/mol) of gaseous alkali astatides (MAt)$_g$.

		LiAt	NaAt	KAt	RbAt	CsAt
	d (Å)[a]	2.476	2.793	3.133	3.262	3.407
(a)	*GBE*	564	492	436	421	413
(b)	ΔH_f	−55	−65	−107	−117	−140
(c)	$\Delta H_f(M^+)_g$	680	603	508	484	452
a + b − c	ΔH_f (At$^-$)$_g$	**−171**	**−177**	**−179**	**−180**	**−179**

Note: Average ΔH_f (At$^-$)$_g$ = −177.2 ± 3.6 kJ/mol.
[a]Liu and Li.[36]

common M (see Tables 1 and 2) as shown in Table S3 and these internuclear distances are given in Table 4.

Using our derived d values for solid and gas phase MAt, their thermodynamic functions may be calculated using Equations (4) and (5) and the empirical parameters in Tables S1 and S2. The results are presented in Tables 3 and 4. Table 3 gives the estimated GBE and ΔH_f for $(MAt)_g$ as well as (in bold) ΔH_f $(At^-)_g$ derived therefrom using Equation (2). Table 4 gives the estimated LBE and ΔH_f for $(MAt)_s$ as well as (in bold) ΔH_f $(At^-)_g$ derived therefrom using Equation (1).

By subtracting the Shannon radii[36] from d of the solid alkali astatides (Table 4) we calculate 2.16 ± 0.07 Å for the crystal radius of At^-, which represents a revision downwards of the value in Ref. 34, (2.32 Å). Our value is in agreement with that in Ref. 36, (2.15 Å).

Our values for LBE are in reasonable agreement with those obtained by Equation (3)[34] and by Ladd and Lee,[50] see Table 3, who use completely different procedures, and this lends great support for the procedures used.

2.4 | Heats of formation of $(At^-)_g$ and $(At^0)_g$; bond strength in $(At_2)_g$ and the importance of spin-orbit coupling

The heat of formation of gaseous At^- can be obtained from Equation (1) using the estimated GBE (MAt) and ΔH_f $(MAt)_g$ and from Equation (2) using the estimated LBE (MAt) and ΔH_f $(MAt)_s$. These values are given in Tables 3 and 4 in bold italics. Noteworthy is the finding that the ΔH_f $(At^-)_g$ values derived from the solid and gaseous thermodynamic estimates agree very well. We derive an average value of ΔH_f $(At^-)_g = -177 \pm 5$ kJ/mol, which represents a revision upwards (i.e., less negative) of some previous estimates (−197, −191, and −179 kJ/mol).[11]

The derived ΔH_f $(At^-)_g$ combined with the measured EA (=233.091 ± 0.007 kJ/mol[18]) leads to a heat of formation of At^0, ΔH_f $(At^0)_g = 56 \pm 5$ kJ/mol, which represents a revision downwards from 92 kJ/mol or 97 kJ/mol.[11] The heat of formation of At_2 is not known, but it is reasonable to propose that it will be larger than that of I_2 (62 kJ/mol) and so we derive an upper limit of 50 kJ/mol for the dissociation energy of At_2, which is considerably less than a previously estimated value of 116 kJ/mol[20] and much less than the bond strength of I_2 (148 kJ/mol). There have been a number of theoretical studies dealing with the bond properties of At_2 (and Ts_2), which have recently been summarized and the most recent compilations are briefly discussed below. From these calculations, it appears that the bond strength of At_2 (and of Ts_2) is considerably reduced by spin-orbit coupling (SOC). According to de Macedo et al.[51] D $(At)_2$ ranges from 39–76 kJ/mol, where the most extensive full relativistic calculations, the four component relativistic calculations, agree very well (61,[52] 61,[53] and 66[51] kJ/mol). Casetti et al.[54] obtain values ranging from 36–114 kJ/mol (excluding one component calculations) and these authors argue that such a situation is "disconcerting and calls for further scrutiny of the appropriate ab initio methodologies." Nevertheless, it would appear that our upper limit (50 kJ/mol) is in good agreement with the full (i.e., including SOC) relativistic calculations but is still below the recommended value of Visscher and Dyall (84 ± 13 kJ/mol).[55] Note that Mitin and Van Wullen[53] obtain from scalar relativistic calculations (i.e., without SOC), a value of 167 kJ/mol, but inclusion of SOC leads to a value of 62 kJ/mol (both B3LYP DK6), making spin-orbit coupling effects larger than the value itself. This is also true for other bond parameters, for example, force constant k of At_2 without SOC is 145 Nm^{-1}, but with SOC it reduces to 73 Nm^{-1}.[56] Such SOC contributions have been termed "spectacular."[57] Also, the internuclear distances in the halogen dimers increase due to SOC: The variation is small (0.04%) for Br_2, substantial (0.7%) for I_2, and large (5.5%) for At_2. Evidence has also been presented[49] that At_2 is part of the "charge-shifted" family, epitomized by F_2.[58] It appears that F_2 and At_2 suffer the same fate, both are destabilized, but for different reasons; F_2 is destabilized because of Pauli repulsion (which according to

TABLE 4 Estimated thermodynamic properties (kJ/mol) of solid alkali astatides $(MAt)_s$.

		LiAt	NaAt	KAt	RbAt	CsAt
	d (Å)[a]	3.117	3.327	3.606	3.744	4.048
(d)	LBE[a]	736	688	636	618	596
	LBE[b]	712	660	613	596	577
	LBE[c]	745	686	636	617	595
	LBE[d]	720	657	615	594	586
(e)	ΔH_f[a]	−225	−257	−308	−316	−328
	ΔH_f[d]	−247	−264	−305	−305	−318
(f)	$\Delta H_f(M^+)_g$	680	603	508	484	452
d + e − f	ΔH_f $(At^-)_g$[a]	**−169**	**−172**	**−180**	**−182**	**−184**
	ΔH_f $(At^-)_g$[d]	−205	−205	−197	−192	−184

Note: Average ΔH_f $(At^-)_g = -177.4 \pm 6.6$ kJ/mol.
[a]This work.
[b]Values ±12, using Equation (3), C = 2,533, ionic crystal radius At^- = 2.32 Å.[34]
[c]Values ±12, using Equation (3), C = 2,533, ionic crystal radius At^- = 2.16 Å, this work.
[d]Ladd and Lee.[50]

Barbosa and Barcelos[59] can also be described as lone pair repulsion), while At_2 is destabilized due to spin-orbit coupling. These matters will be discussed elsewhere.

2.5 | Mass spectrometry- and radio gas-chromatography based experiments: Does At_2 exist?

In the mass spectrometry experiments of Appelman,[60] astatine-211 was synthesized by bombardment of bismuth with 29-MeV α-particles and then distilled from the bismuth on a cooled platinum plate. Next, the astatine was distilled directly from the platinum plate into a Time-of-Flight mass spectrometer. This resulted in only At^+ and no At_2^+ could be detected. However, when a small amount of iodine was co-introduced, peaks appeared for I_2^+ and AtI^+ but not for At_2^+. Similar experiments with bromine and chlorine and astatine led to $AtBr^+$ and $AtCl^+$ only. Appelman was careful to point out that the failure to observe At_2^+ does not allow one to draw definitive conclusions about the equilibrium $2At \rightleftharpoons At_2$. For example, the formation of interhalogens AtX could indicate that the reaction $At_2 + X_2 \rightarrow 2AtX$ is exothermic. This may well be the case as At_2 is highly destabilized by SOC, more so than AtX.[49]

Another way to detect astatine compounds is by radio gas chromatography (R-GC) experiments where At-209 compounds are separated by GC and detected by α-rays from At-209.[61] In this way, AtI and At_2 could be separated and identified. Interestingly, the boiling points of AtI and At_2 could be determined and that of AtI was found to be the mean value of the boiling points of I_2 and At_2, following the general rule for boiling points of the interhalogens.[61]

2.6 | Charge-transfer dissociation energies, D, of the alkali halides, including the astatides

In 1896, Goldstein discovered coloration of alkali halide crystals by UV light, which Przibram later interpreted as arising from neutral alkali atoms formed by electron transfer from the anion to cation.[62] This process ($M^+X^- \rightarrow M^0 + X^0$) also occurs in the gas phase[63] and has since then been the subject of many publications. The energy requirement for these processes for all alkali halides are given in Table 5 and is called the neutral dissociation energy D. The energy needed for

$M^+X^- \rightarrow M^+ + X^-$ (called *GBE* above) may be termed the ionic dissociation energy.[21,22] The difference between *GBE* and D is, see Figure 1:

$$GBE\,(MX) - D\,(MX) = IE_1(M) - EA(X) \qquad (6)$$

and since $IE_1(M) > EA(X)$, *GBE* (MX) will always be larger than D (MX); thus, dissociation of the ionic structure M^+X^- to the *atoms* is always more favorable. Indeed, gas-phase alkali halides are prototypical systems for the study of such charge transfers. These salt molecules have an ionic character at small internuclear distances, but can undergo an avoided crossing at fairly large distances (7.2–9.4 Å) marked by a sharp change in dipole moment of the system.[64]

It can be seen from Table 5, that D decreases in going from LiX to NaX and then it increases again (KX, RbX, CsX). It can be seen from Table 5 that D monotonically decreases for a common M, but the situation appears more complex for common X, where at first D decreases and then it increases again. This has been observed previously.[43] In Figure 4A we have plotted these D values where X is kept constant, together with the *GBE* values. As expected, the *GBE* shows a gradual decline from Li to Cs (and from F to I) because of its inverse relationship with the bond length d. However, for D, it is seen that U-shaped curves result, see Figure 4A. The solution to this somewhat puzzling result is surprisingly trivial when one analyses the reverse process, viz. reaction of M^0 and X^0 to produce [M^+X^-] using a triadic approach[65]: (1) ionization of the alkali atom ($M^0 \rightarrow M^+ + e^-$), (2) electron capture by the halogen atom ($X^0 + e^- \rightarrow X^-$), and finally (3) formation of an ionic bond, $M^+ + X^- \rightarrow MX$. We then obtain (also by rewriting Equation (6)) for $M^0 + X^0 \rightarrow M^+ + X^- \rightarrow MX$:

$$D\,(MX) = -IE_1(M) + EA(X) + GBE\,(MX) \qquad (7)$$

For common X, as is the case in Figure 4A, IE_1(M) and *GBE* (MX) both decrease in the order Li, Na, K, Rb, Cs and subtraction of these quantities yields a U-shape curve. Thus, Equation (7) is highly interpretive, but the underlying assumption, that exactly one electron jumps from M^0 to X^0 may be an idealization.[66] That the gap between *GBE* and D curves is largest for the astatides is a direct consequence of the low EA measured for At^0.

It can also be seen that if M is kept constant, a continuous decline is observed in the order F, Cl, Br, I, At as changes in EA are not as large as changes in IE_1 and more importantly they operate in opposite directions, see Equation (7). It can be seen from Figure 4A that the most stable alkali halide is LiF, whereas the least stable is NaAt.

Also shown in Figure 4A are the force constants, k, taken from Kaya et al.[67] It can be seen that the force constants follow the trend for the dissociations to ions, that is, for the *GBE*, not the trend for the dissociations to neutrals, that is, not for D. This is, of course, as expected for species being ionic near equilibrium distances, because k is the second derivative of the energy at the equilibrium structure with regard to the bond length.
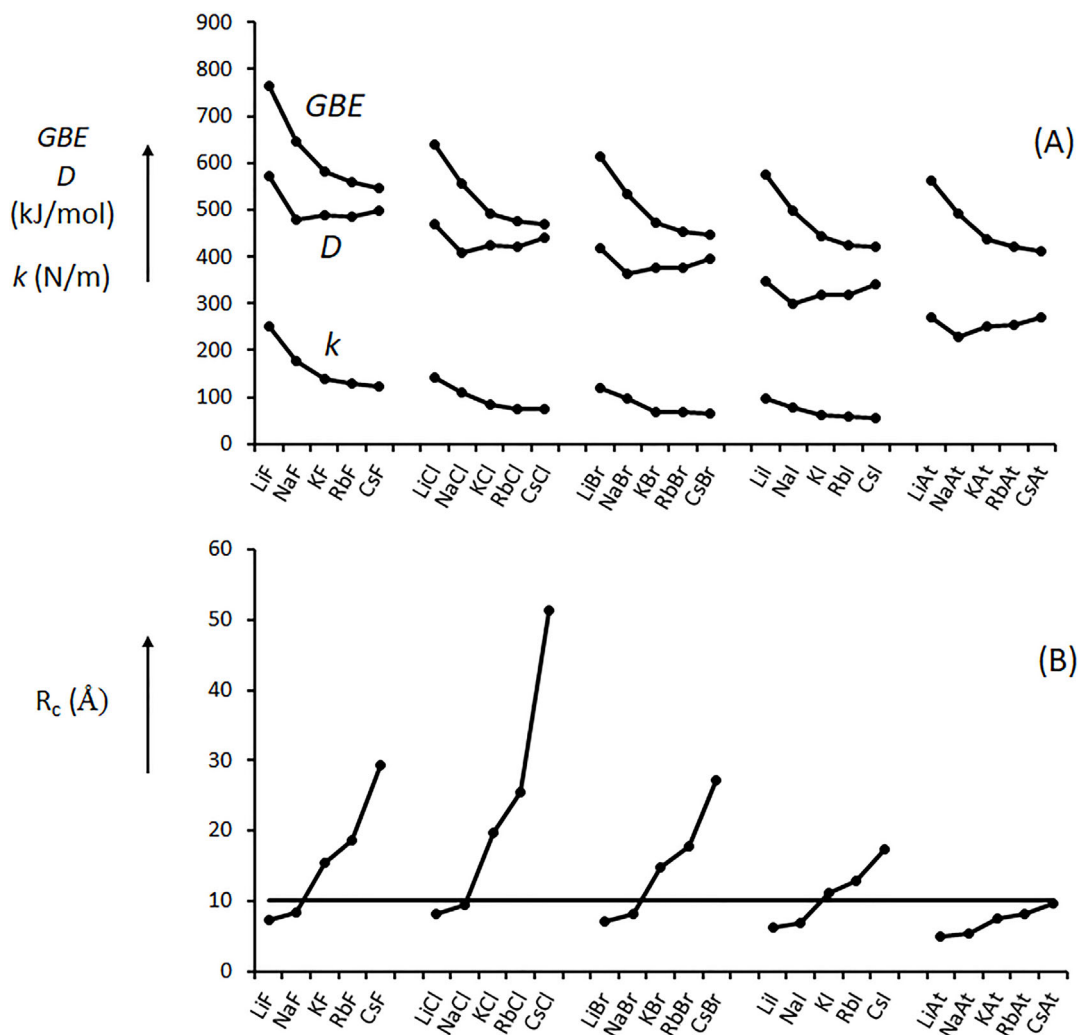
TABLE 5 Gas-phase dissociation energies, D, $(MX)_g \rightarrow M^0 + X^0$.

X\M	Li	Na	K	Rb	Cs
F	573	478	490	484	498
Cl	468	408	424	421	441
Br	417	362	377	377	397
I	346	300	320	318	341
At	269	229	252	254	272

Note: Values in kJ/mol.

—WILEY

FIGURE 4 (A) Gas-phase binding energies (*GBE*, kJ/mol), dissociation energies (*D*, kJ/mol) and force constants (*k*, N/m) for the alkali halides and (B) critical distance for electron transfer, see text.

2.7 | Crossing distances: how do alkali astatides dissociate?

When an alkali halide M^+X^- dissociates to the separated atoms $M^0 + X^0$ then at some internuclear distance (R_c) electron transfer must take place. This process is the archetype[68] of the curve-crossing problem, but for our purposes the following simplification will suffice. The distance R_c at which the potential energy curve for $M^+ + X^-$ would cross the energy of the separated atoms $M^0 + X^0$ can be calculated using the Rittner potential for the ionic state,[64,69–72] which yields (in atomic units):

$$\Delta E_\infty = 1/R_c + \{\alpha(M^+) + \alpha(X^-)\}/2R_c^4 \tag{8}$$

where short distance repulsive terms may be neglected.[64,72]

ΔE_∞ is the energy difference of the ionic ($M^+ + X^-$) and neutral ($M^0 + X^0$) states at infinite separation, $\Delta E_\infty = IE_1(M) - EA(X)$ (=*GBE* (MX) − *D* (MX)) and α are polarizabilities. From Equation (8), R_c may

be obtained iteratively. Because for the alkali halides the ionization energies of M are only slightly larger than the electron affinities of X, the crossing radii are quite large (6–20 Å,[69] 7–10 Å[64]), and so the second term in Equation (8) may be neglected to yield the simple expression:

$$R_c = 1389/\Delta E_\infty \tag{9}$$

R_c in Å, ΔE in kJ/mol, which leads to R_c's being only slightly smaller (for example, for LiCl using Equation (9), R_c = 8.11 Å vs 8.15 Å, iteratively from Equation (8)). Thus the crossing distance is determined almost wholly by $IE_1(M) - EA(X)$ and these quantities are accurately known, also for X = At.

The R_c's calculated from Equation (8) are plotted in Figure 4B (ion polarizabilities from Li et al.,[73] α (At$^-$) from Réal et al.[74]) It can be seen that for alkali halides with small values for $IE_1(M) - EA(X)$ (i.e., for small gaps in Figure 4A, for example CsCl), R_c becomes exceedingly large (51 Å for CsCl[44]), far too large for electron transfer to take place;

as a consequence these species dissociate to ionic products only despite this process requiring more energy ("chemical overshoot").[75,76] (Electronic velocities are about 40 times nuclear velocities[77] and so if the crossing distance is 0.1 Å wide, the electron can only jump 4 Å.) Putting the critical crossing distance at c. 10 Å[64] in Figure 4B, then species above this line dissociate to ions, but species below this line produce atoms.[68] It can be seen that *all* alkali astatides are predicted to produce atoms, not ions, upon dissociation via rapid electron transfer. For example, LiAt will dissociate to atoms at an internuclear separation of only 5.10 Å. The difference between the iodides and astatides is quite remarkable, the crossing in CsAt occurs at a much smaller distance (9.7 Å) than in CsI (17.2 Å), which is a direct consequence of the low measured *EA* (At)[18] compared with *EA* (I), 2.41 eV vs 3.06 eV.

Another way to generate metal atoms from alkali halides is by dissociative electron capture of MX if stray electrons are present: MX + e → M^0 + X$^-$ rather than electron transfer from X$^-$ to M$^+$ as discussed above. However, the enthalpy change for these reactions, which is given by GBE (MX) $- IE_1$(M) $= D$ (MX) $- EA$(X), is positive (endothermic) for all alkali halides, except for NaAt for which the reaction is predicted to be slightly exothermic. That alkali halides anions themselves can be remarkably stable species was first shown by Carlsten et al. in 1976.[78] The expression of Miller et al.,[79] viz. *EA* (MX) $= 114.7 - 9.94 * \alpha(M)/R^2$ (*EA* in kJ/mol), where R is the internuclear distance of MX in Å, allows the estimation of *EA* (NaAt) $= 84$ kJ/mol (α (Na)[80] $= 24.09$ Å^3 and R (NaAt) $= 2.79$ Å, see Table 3), from which ΔH_f (NaAt)$^-$ $= -150$ kJ/mol (using ΔH_f (NaAt) $= -66$ kJ/mol, see Table 4). The energy diagram of the dissociative electron capture by NaAt is given in Figure 5.

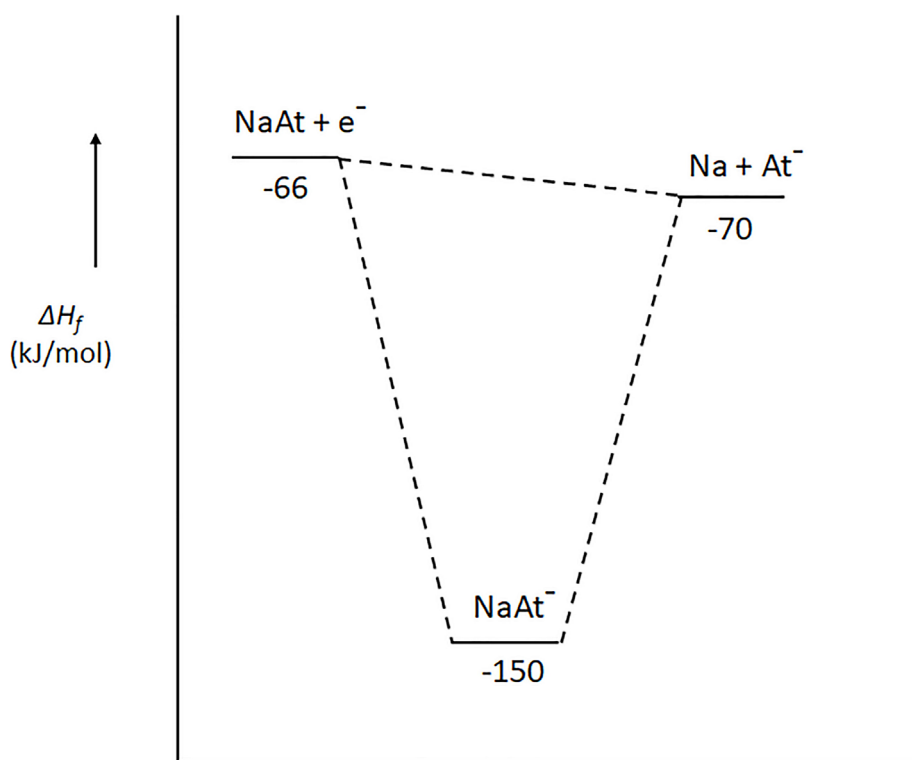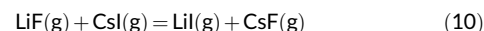## 2.8 | Hard/soft acid/base (HSAB) principle for alkali halides

The double-exchange reaction

$$LiF(g) + CsI(g) = LiI(g) + CsF(g) \qquad (10)$$

has often been used to illustrate the hard/soft acid/base (HSAB) principle: whenever "other effects" (chiefly the strength of the acids and bases) are similar, hard acids (A$_h$) prefer binding to hard bases (B$_h$) and soft acids (A$_s$) prefer binding to soft bases (B$_s$).[81] Thus, the equilibrium for the reaction A$_h$B$_h$ + A$_s$B$_s$ = A$_h$B$_s$ + A$_s$B$_h$ will tend to lie to the left. The Pauling bond equation for the enthalpy change (in eV) for reaction (10) is[82]:

$$\Delta H_{reaction} = 2[\chi_{Cs} - \chi_{Li}][\chi_F - \chi_I] \qquad (11)$$

where χ represents the Pauling electronegativities; this equation would yield $\Delta H_{reaction} = -48$ kJ/mol, hence reaction (10) would be exothermic. However, in reality $\Delta H_{reaction} = +59$ kJ/mol (see Table 1) and so the reaction is in fact endothermic and the equilibrium lies to the left. In general, hard reagents are smaller than soft reagents and so a useful generalization for reactions like (10) is: "small likes small and large likes large."[81] (This principle can also be applied to the solubility of the alkali halides, see later.) This continues for the astatides, where the reaction LiF(g) + CsAt(g) = LiAt(g) + CsF(g) is calculated to be even more endothermic (87 kJ/mol) than reaction (10). This is in agreement with the experimental finding that At is softer than I[18]: the softness S of At (defined as S = 1/(2η)), where η is the hardness

FIGURE 5 Energy diagram for dissociative electron capture by NaAt.

—WILEY

(defined as $\eta = \frac{1}{2}(IE - EA)$; thus, $S = 1/(IE - EA)$), is S (At) = 0.145 eV^{-1}, whereas S(I) = 0.135 eV^{-1}.

2.9 | Sublimation energies of (MAt)$_s$

From the data in Tables 3 and 4, the sublimation energies (SE) of (MAt)$_s$ may be assessed, see Table 6, from $SE = \Delta H_f(g) - \Delta H_f(s)$ or from $SE = LBE - GBE$, see also Figure 1. These values together with those of Brewer[43] are listed in Table S6 and agreement is good. The values for the average SEs for all alkali halides are plotted in Figure 6. The largest sublimation energies are for LiF and NaF, as observed previously,[43] with the prediction that LiAt has the lowest sublimation energy.

2.10 | Melting temperatures of the alkali astatides

The melting temperature, T_m, is an important physicochemical property of ionic crystals. For many substances T_m is an identifying characteristic and a criterion of the purity of crystals. Melting temperatures are particularly difficult to calculate; in free energy methods,[83] the free energy difference between the two phases is calculated and the melting temperature is defined as the temperature at which the free energy difference between the two phases is zero, which is computationally demanding: differences of 4 kJ/mol can result in errors of as much as 100 K. This is not unlike the calculation of pK_a values in solution where such differences give an error of 1 pK_a unit.[84]

It is known[85] that with a decrease in the crystal lattice energy, the melting temperature decreases. Thus, since the LBE's show an
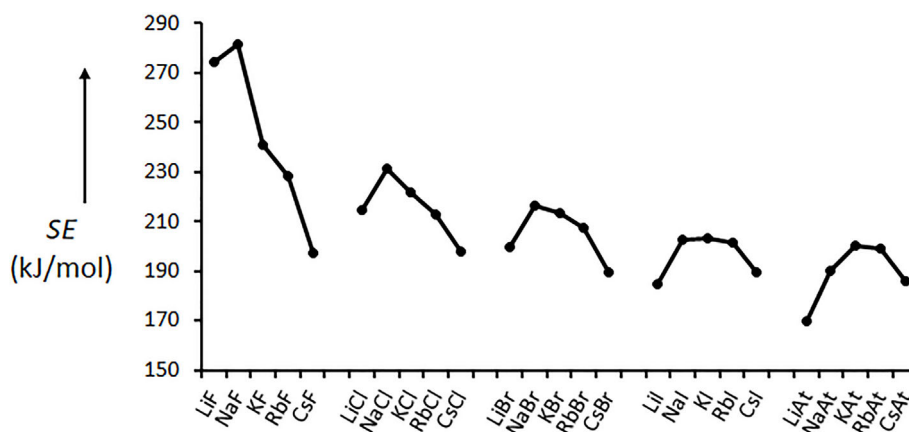
inverse proportionality with d, it is expected that the T_m's will also be inversely proportional to d. However, it is known that the T_m's of the lithium halides are much smaller than predicted on the basis of their d values[31] and it is very difficult to find a generalized equation relating T_m with d. Indeed, an equation analogous to Equation (3) leads to the T_m's of the lithium halides being c. 250 K too large. Oshchapovskii[35] has used a modified equation, which produces T_m reasonably well, but discrepancies up to 80 K still persist. However, an important observation made by Oshchapovskii is that T_m is linearly related with LBE for all alkali halides provided (as was the case with other relationships, see above) that the alkali cation is kept constant and so T_m will be linear with 1/d for all five subfamilies. This is indeed the case and the empirical constants for $T_m = \alpha/d + \beta$, together with R^2 are given in Table S4 for alkali halides with common metal ion. (The correlation is not as good as for LBE with 1/d, compare Table 3.) The T_m values for MAt found by extrapolation are given in Table 7, together with the calculated values by Oshchapovskii. Our estimated melting temperatures for RbAt and CsAt agree with the calculations of Oshchapovskii, but the discrepancies for the others, especially for NaAt, are quite large. However, the calculated T_m values for some alkali halides, notably NaCl, also deviate from the experimental values.[35]

The melting temperatures follow an inverted U-shaped curve for a common anion, paralleling the behavior of the other alkali halides, see Figure 7. It can be seen from this Figure, that our estimated values of T_m for the alkali astatides more closely follow the experimental T_m values of the other alkali halides, especially for the bromides and iodides. Also shown in Figure 7 are the melting temperatures predicted by the WBK (Wang-Buckingham) method using polarized force fields.[86]

2.11 | Hydration enthalpy and ionic radius of At$^-$: is the largest alkali halide, CsAt, insoluble in water?

The solubility of MX in water depends on the lattice energy of MX and the hydration energies of its ions M$^+$ and X$^-$.[87] Kaya and de Farias[88] have pointed toward a correlation between the lattice binding energy (LBE) and the sum of hydration enthalpies of M$^+$ and X$^-$ (=

TABLE 6 Estimated sublimation energies (kJ/mol) of alkali astatides MAt.

	LiAt	NaAt	KAt	RbAt	CsAt
d–a from Tables 3 and 4	171	194	200	198	184
b–e from Tables 3 and 4	170	186	200	200	187

FIGURE 6 Sublimation energies (kJ/mol) for the alkali halides.

TABLE 7 Melting temperatures T_m (K) for the alkali astatides, estimated by extrapolation (this work), and from the calculations of Oshchapovskii.[35]

	LiAt	NaAt	KAt	RbAt	CsAt
This work	722	918	954	920	889
Oshchapovskii[35]	652	791	869	924	894

$-\Sigma\Delta H_{aq}$), as can also be inferred from Table 1. Since LBE is proportional to $1/d$, we expect $-\Sigma\Delta H_{aq}$ too to be proportional to $1/d$. Next, consider the processes whereby gaseous or solid MX are dissolved in water:
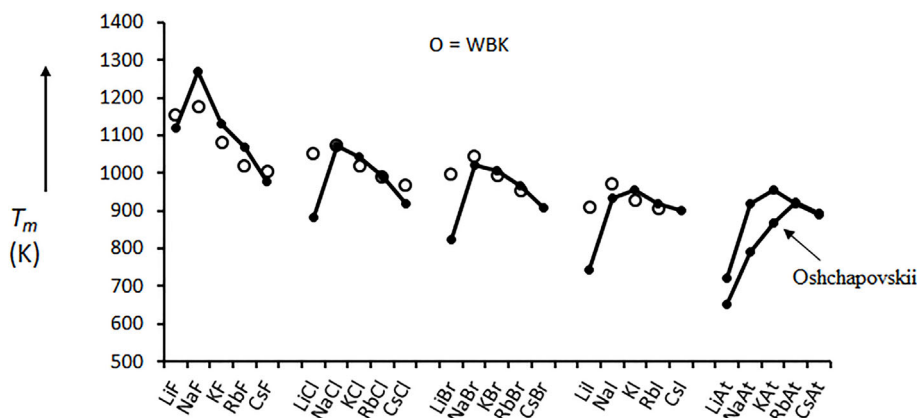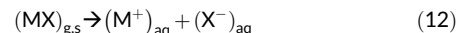
$$(MX)_{g,s} \rightarrow (M^+)_{aq} + (X^-)_{aq} \qquad (12)$$

FIGURE 7 Melting temperatures (T_m, K) of the alkali halides. Calculations for the metal astatides by Oshchapovskii[35] as indicated. Open circles from WBK calculations.
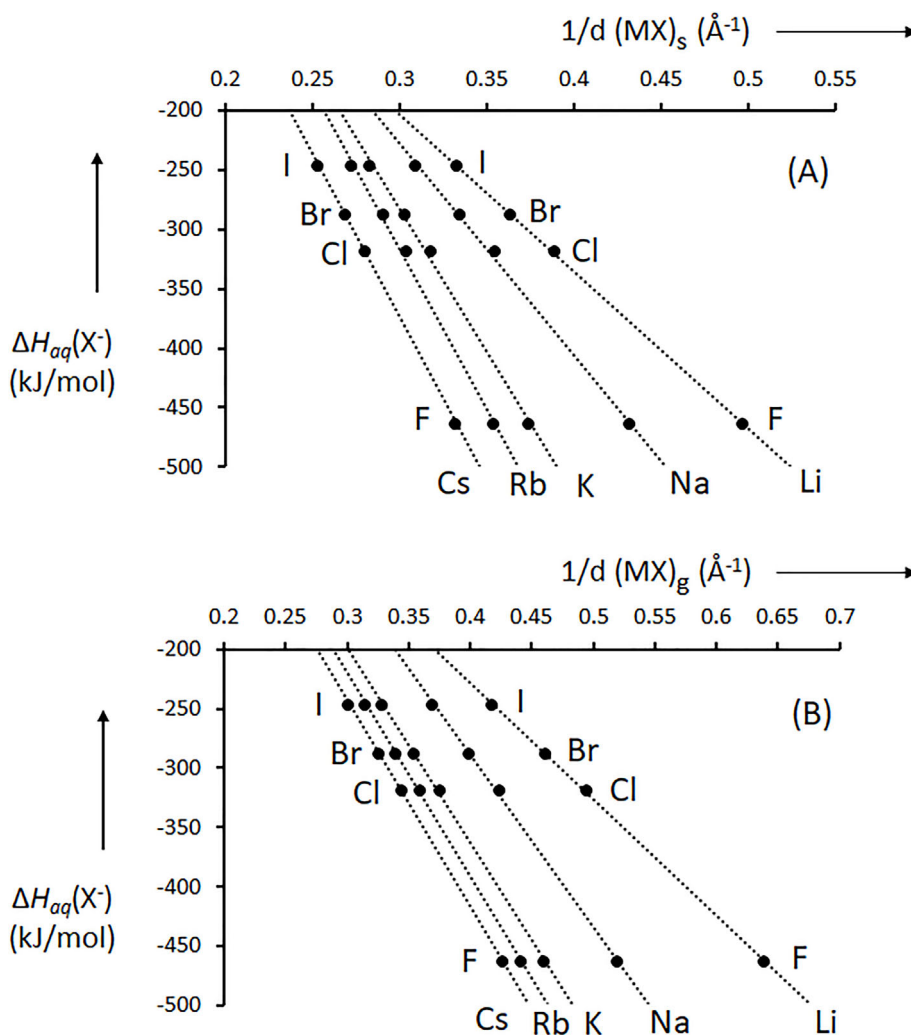

FIGURE 8 Hydration enthalpies of the halide anions ($\Delta H_{aq}(X^-)$, kJ/mol) as a function of the reciprocal bond length $1/d$ (Å^{-1}) of solid (A) and gaseous (B) alkali halides.

TABLE 8 Difference in hydration enthalpies ($\Delta H_{hyd}{}^{X \to Y}$) and hydration free energies ($\Delta G_{hyd}{}^{X \to Y}$) of the halide anions.

	$\Delta H_{hyd}{}^{X \to Y}$		$\Delta G_{hyd}{}^{X \to Y}$		
	Exp (Housecroft and Jenkins[30])	Exp (Housecroft and Jenkins[30])	Rueda-Espinosa et al.[90]	Rueda-Espinosa et al.[90]	Real et al.[74]
$F^- \to Cl^-$	144	125	118	118	113
$Cl^- \to Br^-$	31	26	21	8	28
$Br^- \to I^-$	42	35	31	29	39
$I^- \to At^-$	17 ± 2 (this work)	-	3	18	6

Note: Values in kJ/mol.

For a common ion M^+ we then expect the following relationship:

$$\Delta H_{aq}(X^-) = \alpha/d + \beta \qquad (13)$$

where d is the gaseous or solid internuclear distance. This relationship allows the estimation of the hydration energy of the astatide anion, ΔH_{aq} (At$^-$). Indeed, we find very good correlations between $\Delta H_{aq}(X^-)$ and d for the gaseous and solid alkali halides, see Figure 8 (the enthalpies of hydration (kJ/mol) for F$^-$ (−463.7), Cl$^-$ (−319.5), Br$^-$ (−288.7) and I$^-$ (−246.8) were taken from Housecroft and Jenkins[30] with reference to $\Delta H_{aq}(H^+) = -1150.1$ kJ/mol[89]). The empirical constants of Equation (13) are given in Tables S5 and S6. From Table S5 and using d (MAt)$_g$ from Table 3, we find ΔH_{aq} (At$^-$) = −231 ± 2 kJ/mol and from Table S6, using d (MAt)$_s$ from Table 4, we find ΔH_{aq} (At$^-$) = −229 ± 1 kJ/mol, leading to ΔH_{aq} (At$^-$) = −230 ± 2 kJ/mol. Note that this value is only 17 ± 2 kJ/mol less negative than the hydration enthalpy of I$^-$ and so the hydration energies of I$^-$ and At$^-$ are predicted to be very close. Indeed, our value for ΔH_{aq} (At$^-$) = −230 ± 2 kJ/mol compares very favorably with values recently obtained from Molecular Dynamics (MD) calculations.[74,90] To avoid problems with some of the corrections necessary in the proper calculation of ion hydration free energies, differences in hydration energies are reported, see Table 8. It can be seen that such calculations predict that the solvation of astatide in bulk water is very close to that of iodide, in good agreement with our results.

Recent work on micro-solvation on the halide anions confirm these results.[91,92] In Table 9, we collect the difference in micro-hydration energies of the halide ions for six water molecules.

It can be seen that these micro-hydration energies of At$^-$ are only 5 kJ/mol smaller than those of I$^-$. The derived ΔH_{aq} (At$^-$) allows the estimation of the ionic (Goldschmidt) radius of At$^-$, R (At$^-$). Following the procedure of Housecroft and Jenkins,[30] a plot of $\Delta H_{aq}(X^-)$ (X = F, Cl, Br, I) versus 1/R(X$^-$) gives a straight line (R^2 = 0.99995) from which, by extrapolation, R (At$^-$) = 2.33 ± 0.01 Å, a value larger than the crystal radius (2.16 Å, see above), paralleling the behavior of the other halogens. Our derived ionic radius of At$^-$ fits nicely with the calculated atomic radius of At, R (At^0) = 1.52 Å[51] following the observation that for the halogens R (X$^-$) − R (X^0) = 0.78 ± 0.02 Å (values for R(X^0) taken from Cordero et al.[93] and values for R(X$^-$) taken from

TABLE 9 Difference in micro-hydration enthalpies ($\Delta H_{hyd}{}^{X \to Y}$) and micro-hydration free energies ($\Delta G_{hyd}{}^{X \to Y}$) of the halide anions for six water molecules.

	$\Delta H_{hyd}{}^{X \to Y}$		$\Delta G_{hyd}{}^{X \to Y}$	
	92		92	91
$F^- \to Cl^-$				108
$Cl^- \to Br^-$				20
$Br^- \to I^-$	23		22	21
$I^- \to At^-$	5		5	5

Note: Values in kJ/mol.

Housecroft and Jenkins[30]). Our value for R (At$^-$) is significantly smaller than that estimated by Chang et al, R (At$^-$) = 2.59 ± 0.09 Å.[94]

Differences in solubilities of the alkali halides may be due to differences in their lattice energies or differences in hydration energies of their ions. The free energy change of the process lattice to hydrated ions determines the solubility of MX.

The enthalpy of dissolution (or enthalpy of solution, ΔH_s) for the process $(MX)_s \to (M^+)_{aq} + (X^-)_{aq}$ is given by $\Delta H_s = LBE$ (MX) $+ \Sigma \Delta H_{aq}$, see Table 1 and represents the difference of two very large and similar quantities. The free energy of dissolution (ΔG_s) of the alkali halides is given by $\Delta G_s = \Delta H_s - T\Delta S_s$. It was shown by Ladd and Lee[87] that all alkali halides have negative values for ΔG_s except LiF, which indeed is only sparingly soluble in water. It is very difficult to find a quantitative relation between the solubility (*m*) and ΔG_s for all alkali halides, but we can indicate what the solubilities of the alkali astatides might be by way of considering NaAt and CsAt. In Table 10, we have collected the solvation enthalpies, the solvation free energies and the solubilities (in mol/kg) of the sodium and cesium halides. The enthalpy of dissolution (ΔH_s) for MAt was obtained from $\Delta H_s = LBE$ (MAt) + $\Sigma \Delta H_{aq}$ (MAt), where LBE (MAt) is given in Table 4 and $\Sigma \Delta H_{aq}$ (MAt) = $\Delta H_{aq}(M^+) + \Delta H_{aq}$ (At$^-$), where ΔH_{aq} (Na$^+$) = −463 kJ/mol,[30] ΔH_{aq} (Cs$^+$) = −331 kJ/mol[30] and ΔH_{aq} (At$^-$) = −230 kJ/mol, see above.

It can be seen that the relative solubilities of the sodium halides, including NaAt, are chiefly determined by entropy effects and so, considering the trend in these, NaAt will be very soluble in water. (For the sodium halides, there is a very delicate balance between LBE and $-\Sigma \Delta H_{aq}$, see Table 1.) By contrast, again by considering the trends of

MX	m^a	ΔH_s^b	$T\Delta S_s^b$	ΔG_s^b	MX	m^a	ΔH_s^b	$T\Delta S_s^b$	ΔG_s^b
NaF	1	0	−3	+3	CsF	38	−37	+14	−51
NaCl	6	+4	+13	−9	CsCl	11	+18	+27	−9
NaBr	9	−1	+16	−17	CsBr	6	+26	+28	−2
NaI	12	−8	+23	−31	CsI	3	+33	+34	−1
NaAt		−5[c]			CsAt		+35[c]		

TABLE 10 Solubilities, m (mol/kg at 298.15 K) and thermodynamic functions relating to energies of solution for the sodium and cesium halides (kJ/mol).

[a]Haynes.[95]
[b]Ladd and Lee.[87]
[c]This work.

ΔH_s and ΔG_s in Table 10, it might very well be that ΔG_s (CsAt) becomes positive and thus CsAt may be only sparingly soluble in water, like LiF ($m = 0.05$ mol/kg). It is of interest to note[95] that the least soluble alkali halides are LiF, NaF, CsI (and very likely CsAt), with RbF and CsF being the most soluble, which is in line with the generalization "small likes small and large likes large."[81,96]

3 | SUMMARY

The bond length in gaseous and solid alkali halides is a good descriptor for various of their thermodynamic and physicochemical properties. Good linear correlations are found provided that the metal cation is kept constant. Such correlations permit the estimation of thermodynamic and physicochemical properties (solid and gas-phase heats of formation, sublimation energies, lattice binding energies, gas-phase dissociation energies and melting temperatures) for the alkali astatides (MAt) and these are compared with previous estimates and calculations. All gas-phase alkali astatides are predicted to dissociate to atoms, not ions, by rapid charge transfer at relatively small internuclear distances (<10 Å, 9.7 Å for CsAt). By comparison, CsI dissociates to ions because for CsI charge transfer is calculated to take place at a significantly larger distance (circa 17 Å).

Using the Born-Haber cycle, ΔH_f (At$^-$)$_g$ is assessed as −177 ± 5 kJ/mol, which represents a revision of some earlier estimates (−197, −191, and −179 kJ/mol). Based on the recently measured electron affinity of At^0, we derive ΔH_f (At^0)$_g$ = 56 ± 5 kJ/mol, which represents a significant revision of earlier estimates (92 and 97 kJ/mol). For At$_2$ we derive an upper limit for the dissociation energy of 50 kJ/mol, which is considerably less than a previously estimated value of 116 kJ/mol and much less than the bond strength of I$_2$ (148 kJ/mol). Our results are in agreement with published full relativistic calculations that predict the bond strength of At$_2$ (and Ts$_2$) to be greatly reduced by spin-orbit coupling.

The hydration enthalpy of At$^-$ is estimated to be −230 ± 2 kJ/mol (using ΔH_{aq}(H$^+$) = −1150.1 kJ/mol), which is only 17 ± 2 kJ/mol less negative than the hydration enthalpy of I$^-$, in good agreement with recent molecular dynamics calculations.

DATA AVAILABILITY STATEMENT

The data that supports the findings of this study are available in the supplementary material of this article

ORCID

Peter C. Burgers https://orcid.org/0000-0003-3418-8438

REFERENCES

1. Si R, Fischer CF. Electron affinities of at and its homologous elements cl, Br, and I. *Phys Rev A*. 2018;98(5):052504. doi:10.1103/PhysRevA.98.052504
2. Guérard F, Maingueneau C, Liu L, et al. Advances in the chemistry of astatine and implications for the development of radiopharmaceuticals. *Acc Chem Res*. 2021;54(16):3264-3275. doi:10.1021/acs.accounts.1c00327
3. Lindegren S, Albertsson P, Bäck T, Jensen H, Palm S, Aneheim E. Realizing clinical trials with Astatine-211: the chemistry infrastructure. *Cancer Biother Radiopharm*. 2020;35(6):425-436. doi:10.1089/cbr.2019.3055
4. Pouget JP, Constanzo J. Revisiting the radiobiology of targeted alpha therapy. *Front Med (Lausanne)*. 2021;8:692436. doi:10.3389/fmed.2021.692436
5. Bloomer WD, McLaughlin WH, Neirinckx RD, et al. Astatine-211--tellurium radiocolloid cures experimental malignant ascites. *Science*. 1981;212(4492):340-341. doi:10.1126/science.7209534
6. Zalutsky MR, Reardon DA, Akabani G, et al. Clinical experience with alpha-particle emitting 211At: treatment of recurrent brain tumor patients with 211At-labeled chimeric antitenascin monoclonal antibody 81C6. *J Nucl Med*. 2008;49(1):30-38. doi:10.2967/jnumed.107.046938
7. Vaidyanathan G, Zalutsky MR. Applications of 211At and 223Ra in targeted alpha-particle radiotherapy. *Curr Radiopharm*. 2011;4(4):283-294. doi:10.2174/1874471011104040283
8. Gustafsson AM, Bäck T, Elgqvist J, et al. Comparison of therapeutic efficacy and biodistribution of 213Bi- and 211At-labeled monoclonal antibody MX35 in an ovarian cancer model. *Nucl Med Biol*. 2012;39(1):15-22. doi:10.1016/j.nucmedbio.2011.07.003
9. Tadashi W, Kazuko K-N, Yuwei L, et al. Enhancement of astatine-211 uptake via the sodium iodide symporter by the addition of ascorbic acid in targeted alpha therapy of thyroid cancer. *J Nucl Med*. 2019; jnumed.118.222638.
10. Liu Y, Watabe T, Kaneda-Nakashima K, et al. Preclinical evaluation of radiation-induced toxicity in targeted alpha therapy using [211At] NaAt in mice: a revisit. *Transl Oncol*. 2020;13(4):100757. doi:10.1016/j.tranon.2020.100757
11. Vasáros L, Berei K. General Properties of Astatine. In: Berei K, Eberle SH, Kirby HW, et al., eds. *At astatine*. Springer; 1985:107. doi:10.1007/978-3-662-05868-8_5
12. Zollweg RJ. Electron affinities of the heavy elements. *J Chem Phys*. 2003;50(10):4251-4261. doi:10.1063/1.1670890
13. Finney BA, Peterson KA. Beyond chemical accuracy in the heavy p-block: the first ionization potentials and electron affinities of Ga-Kr, in-Xe, and Tl-Rn. *J Chem Phys*. 2019;151(2):024303. doi:10.1063/1.5110174

14. Sen KD, Schmidt PC, Weiss A. Slater transition state calculations of electron affinity of heavy atoms. *J Chem Phys*. 1981;75(2):1037-1038. doi:10.1063/1.442069

15. Li J, Zhao Z, Andersson M, Zhang X, Chen C. Theoretical study for the electron affinities of negative ions with the MCDHF method. *J Phys B-At Mol Opt Phys*. 2012;45(16):45. doi:10.1088/0953-4075/45/16/165004

16. Borschevsky A, Pašteka LF, Pershina V, Eliav E, Kaldor U. Ionization potentials and electron affinities of the superheavy elements 115--117 and their sixth-row homologues bi, Po, and at. *Phys Rev A*. 2015;91(2):020501. doi:10.1103/PhysRevA.91.020501

17. Sergentu D-C, David G, Montavon G, Maurice R, Galland N. Scrutinizing "invisible" astatine: a challenge for modern density functionals. *J Comput Chem*. 2016;37(15):1345-1354. doi:10.1002/jcc.24326

18. Leimbach D, Karls J, Guo Y, et al. The electron affinity of astatine. *Nat Commun*. 2020;11(1):3824. doi:10.1038/s41467-020-17599-2

19. Yungman VS, Glushko VP, Medvedev VA, Gurvich LV. *Thermal constants of substances*. Wiley; 1999.

20. Kiser RW. Estimation of the ionization potential and dissociation energy of molecular astatine. *J Chem Phys*. 1960;33(4):1265-1266. doi:10.1063/1.1731380

21. Srivastava BN. *Heat of ionic dissociation of iodides of rubidium and lithium and electron affinity of iodine*. Vol. 4; 1938:365.

22. Srivastava BN. *Heat of ionic dissociation of the chloride and bromide of rubidium*. Vol. 5; 1939:313.

23. Nasar A. Correlation between standard enthalpy of formation, structural parameters and ionicity for alkali halides. *J Serb Chem Soc*. 2013;78(2):241-253. doi:10.2298/JSC120113049N

24. Sirdeshmukh DB, Sirdeshmukh L, Subhadra KG. *Alkali halides: a handbook of physical properties*. Springer; 2001. doi:10.1007/978-3-662-04341-7

25. *NIST chemistry WebBook*, https://janaf.nist.gov/ Accessed 2023

26. Wagman DD, Evans WH, Parker VB, et al. NBS tables of chemical thermodynamic properties. *J Phys Chem Ref Data Monogr*. 1982;11.

27. Kaya S, Kaya C. A simple method for the calculation of lattice energies of inorganic ionic crystals based on the chemical hardness. *Inorg Chem*. 2015;54(17):8207-8213. doi:10.1021/acs.inorgchem.5b00383

28. Morris DFC. The lattice energies of the alkali halides. *Acta Crystallogr*. 1956;9(2):197-198. doi:10.1107/S0365110X56000498

29. Woodcock LV. Interionic pair potentials in the alkali metal halides. *J Chem Soc Faraday Trans 2: Molec Chem Phys*. 1974;70:1405.

30. Housecroft CE, Brooke Jenkins HD. Absolute ion hydration enthalpies and the role of volume within hydration thermodynamics. *RSC Adv*. 2017;7(45):27881-27894. doi:10.1039/C6RA25804B

31. Rosseinsky DR. Electrode potentials and hydration energies. Theories and correlations. *Chem Rev*. 1965;65(4):467-490. doi:10.1021/cr60236a004

32. Leung W-P, Chan Y-C. *Alkali metals: inorganic chemistry, encyclopedia of inorganic and bioinorganic chemistry*; 2014:1. doi:10.1002/9781119951438.eibc0003.pub2

33. Gopikrishnan CR, Jose D, Datta A. Electronic structure, lattice energies and born exponents for alkali halides from first principles. *AIP Adv*. 2012;2(1):012131. doi:10.1063/1.3684608

34. Oshchapovskii VV. Interpolation determination of the lattice energy of ionic crystals within the framework of stereoatomic model. *Russ J General Chem*. 2008;78(4):532-542. doi:10.1134/S1070363208040051

35. Oshchapovskii VV. A new method of calculation of the melting temperatures of crystals of group 1A metal halides and francium metal. *Russ J Inorg Chem*. 2014;59(6):561-567. doi:10.1134/S0036023614060163

36. Liu J-B, Schwarz WHE, Li J. On two different objectives of the concepts of ionic radii. *Chem A Eur J*. 2013;19(44):14758-14767. doi:10.1002/chem.201300917

37. De Farias R, Kaya S. Lattice energies for groups 1 and 2 halides from absolute hardness. *Cumhuriyet Sci J*. 2018;39(1):192-195. doi:10.17776/csj.345660

38. Castro E, Toropova A, Toropov A, Mukhamedjanova V. QSPR modeling of metal halides lattice enthalpies. *Anales Asoc Quimica Argentina*. 2006;94:105.

39. Hargittai M. Molecular structure of metal halides. *Chem Rev*. 2000;100(6):2233-2302. doi:10.1021/cr970115u

40. Irikura KK. Experimental vibrational zero-point energies: diatomic molecules. *J Phys Chem Ref Data Monogr*. 2007;36(2):389-397. doi:10.1063/1.2436891

41. Lias SG, Bartmess J, Liebman JF, Holmes J, Levin RD, Mallard G. Gasphase ion and neutral thermochemistry. *J Phys Chem Ref Data (Suppl)*. 1988;1:1.

42. Huber KP, Herzberg G. Constants of diatomic molecules. In: Huber KP, Herzberg G, eds. *Molecular spectra and molecular structure: IV constants of diatomic molecules*. Springer US; 1979:8. doi:10.1007/978-1-4757-0961-2_2

43. Brewer L, Brackett E. The dissociation energies of gaseous alkali halides. *Chem Rev*. 1961;61(4):425-432. doi:10.1021/cr60212a004

44. Su TMR, Riley SJ. Alkali halide photofragment spectra. I. Alkali iodide bond energies and excited state symmetries at 266 nm. *J Chem Phys*. 1979;71(8):3194-3202. doi:10.1063/1.438766

45. Su TMR, Riley SJ. Alkali halide photofragment spectra. III. Alkali chloride bond energies and excited state symmetries at 266 nm. *J Chem Phys*. 1980;72(12):6632-6636. doi:10.1063/1.439121

46. Su TMR, Riley SJ. Alkali halide photofragment spectra. II. Alkali bromide bond energies and excited state symmetries at 266 nm. *J Chem Phys*. 1980;72(3):1614-1622. doi:10.1063/1.439360

47. van Veen N, de Vries M, Vries AE. Accurate determination of the dissociation energies of alkali halides. *Chem Phys Lett*. 1979;64(2):213-215. doi:10.1016/0009-2614(79)80498-4

48. Langhoff SR, Bauschlicher CW, Partridge H. Theoretical Dissociation Energies for Ionic Molecules. In: Bartlett RJ, ed. *Comparison of ab initio quantum chemistry with experiment for small molecules*. Springer; 1985:357. doi:10.1007/978-94-009-5474-8_13

49. Graton J, Rahali S, Le Questel J-Y, Montavon G, Pilmé J, Galland N. Spin–orbit coupling as a probe to decipher halogen bonding. *Phys Chem Chem Phys*. 2018;20(47):29616-29624. doi:10.1039/C8CP05690K

50. Ladd MFC, Lee WH. Lattice energies of the rarer akali halides. *J Inorg Nuclear Chem*. 1961;20(1-2):163-165. doi:10.1016/0022-1902(61)80476-4

51. de Macedo LGM, Neves ER, de Oliveira Só YA, Gargano R. Relativistic four-component potential energy curves for the lowest 23 covalent states of molecular astatine (At2). *Spectrochim Acta A Mol Biomol Spectrosc*. 2021;245:118869. doi:10.1016/j.saa.2020.118869

52. Visscher L. Approximate molecular relativistic Dirac-Coulomb calculations using a simple coulombic correction. *Theor Chem Acc*. 1997;98(2-3):68-70. doi:10.1007/s002140050280

53. Mitin AV, van Wüllen C. Two-component relativistic density-functional calculations of the dimers of the halogens from bromine through element 117 using effective core potential and all-electron methods. *J Chem Phys*. 2006;124(6):064305. doi:10.1063/1.2165175

54. Casetti V, MacLean J, Ayoub A, Fredericks R, Adamski J, Rusakov A. Investigating the heaviest halogen: lessons learned from modeling the electronic structure of astatine's small molecules. *J Phys Chem a*. 2022;127(1):46-56. doi:10.1021/acs.jpca.2c06039

55. Visscher L, Dyall K. Relativistic and correlation effects on molecular properties. I. The dihalogens F2, Cl2, Br2, I2, and At2. *Chem Phys*. 1996;104:9040.

56. Pilmé J, Renault E, Bassal F, Amaouch M, Montavon G, Galland N. QTAIM analysis in the context of quasirelativistic quantum calculations. *J Chem Theory Comput*. 2014;10(11):4830-4841. doi:10.1021/ct500762n

57. Zhao L, Pan S, Holzmann N, Schwerdtfeger P, Frenking G. Chemical bonding and bonding models of main-group compounds. *Chem Rev*. 2019;119(14):8781-8845. doi:10.1021/acs.chemrev.8b00722

58. Shaik S, Danovich D, Galbraith JM, Braïda B, Wu W, Hiberty PC. Charge-shift bonding: a new and unique form of bonding. *Angew Chem Int Ed*. 2020;59(3):984-1001. doi:10.1002/anie.201910085

59. Barbosa A, Barcelos A. The electronic structure of the F2, Cl2, Br 2 molecules: the description of charge-shift bonding within the generalized valence bond ansatz. *Theor Chem Accounts*. 2009;122(1-2):51-66. doi:10.1007/s00214-008-0484-x

60. Appelman EH, Sloth EN, Studier MH. Observation of astatine compounds by time-of-flight mass spectrometry. *Inorg Chem*. 1966;5(5):766-769. doi:10.1021/ic50039a016

61. Otozai K, Takashi N. Estimation of the chemical form and the boiling point of elementary astatine by radiogaschromatography. *Radiochim Acta*. 1982;31(3-4):201-204. doi:10.1524/ract.1982.31.34.201

62. Rabinowitch E. Electron transfer spectra and their photochemical effects. *Rev Mod Phys*. 1942;14(2-3):112-131. doi:10.1103/RevModPhys.14.112

63. Bender CJ. Theoretical models of charge-transfer complexes. *Chem Soc Rev*. 1986;15(4):475. doi:10.1039/cs9861500475

64. Giese TJ, York DM. Complete basis set extrapolated potential energy, dipole, and polarizability surfaces of alkali halide ion-neutral weakly avoided crossings with and without applied electric fields. *J Chem Phys*. 2004;120(17):7939-7948. doi:10.1063/1.1690232

65. Maksić ZB, Kovačević B, Vianello R. Advances in determining the absolute proton affinities of neutral organic molecules in the gas phase and their interpretation: a theoretical account. *Chem Rev*. 2012;112(10):5240-5270. doi:10.1021/cr100458v

66. Maksić ZB, Vianello R. Quest for the origin of basicity: initial vs final state effect in neutral nitrogen bases. *J Phys Chem A*. 2002;106(2):419-430. doi:10.1021/jp013296j

67. Kaya S, Kaya C, Obot IB, Islam N. A novel method for the calculation of bond stretching force constants of diatomic molecules. *Spectrochim Acta A Mol Biomol Spectrosc*. 2016;154:103-107. doi:10.1016/j.saa.2015.10.030

68. Ewing JJ, Milstein R, Berry RS. Curve crossing in collisional dissociation of alkali halide molecules. *J Chem Phys*. 1971;54(4):1752-1760. doi:10.1063/1.1675082

69. Werner HJ, Meyer W. MCSCF study of the avoided curve crossing of the two lowest $1\Sigma+$ states of LiF. *J Chem Phys*. 1981;74(10):5802-5807. doi:10.1063/1.440893

70. Brumer P, Karplus M. Perturbation theory and ionic models for alkali halide systems. I Diatomics. *J Chem Phys*. 2003;58(9):3903-3918. doi:10.1063/1.1679747

71. Hati S, Datta B, Datta D. Polarizability of an ion in a molecule. Applications of Rittner's model to alkali halides and hydrides revisited. *J Phys Chem*. 1996;100(51):19808-19811. doi:10.1021/jp960945w

72. Sousa C, Domínguez-Ariza D, de Graaf C, Illas F. Electric field effects on the ionic-neutral curve crossing of alkali halide molecules. *J Chem Phys*. 2000;113(22):9940-9947. doi:10.1063/1.1323264

73. Li M, Zhuang B, Lu Y, Wang Z-G, An L. Accurate determination of ion polarizabilities in aqueous solutions. *J Phys Chem B*. 2017;121(26):6416-6424. doi:10.1021/acs.jpcb.7b04111

74. Réal F, Gomes ASP, Martínez YOG, et al. Structural, dynamical, and transport properties of the hydrated halides: how do at− bulk properties compare with those of the other halides, from F− to I−? *J Chem Phys*. 2016;144(12):124513. doi:10.1063/1.4944613

75. Coplan M, Cernoch T, Berry RS. Chemical overshoot: thermal dissociation of alkali halide molecules. *Phys Fluids*. 1969;12(5):I-I-119. doi:10.1063/1.1692589

76. Berry RS, Cernoch T, Coplan M, Ewing JJ. Inverted population in dissociation of CsBr molecules. *J Chem Phys*. 1968;49(1):127-134. doi:10.1063/1.1669797

77. Berry RS. Interaction of vibrational and electronic motion in alkali halide molecules. *J Chem Phys*. 1957;27(6):1288-1295. doi:10.1063/1.1743993

78. Carlsten JL, Peterson JR, Lineberger WC. Binding of an electron by the field of a molecular dipole — LiCl−. *Chem Phys Lett*. 1976;37(1):5-8. doi:10.1016/0009-2614(76)80148-0

79. Miller T, Leopold D, Murray K, Lineberger W. Electron affinities of the alkali halides and the structure of their negative ions. *J Chem Phys*. 1986;85(5):2368-2375. doi:10.1063/1.451091

80. Schwerdtfeger P, Nagle JK. 2018 table of static dipole polarizabilities of the neutral elements in the periodic table*. *Molecular Physics*. 2019;117(9-12):1200-1225. doi:10.1080/00268976.2018.1535143

81. Ayers PW, Parr RG, Pearson RG. Elucidating the hard/soft acid/base principle: a perspective based on half-reactions. *J Chem Phys*. 2006;124(19):194107. doi:10.1063/1.2196882

82. Pearson RG. Failure of Pauling's bond energy equation. *Chem Commun (Camb)*. 1968;(2):65. doi:10.1039/c19680000065

83. DeFever RS, Wang H, Zhang Y, Maginn EJ. Melting points of alkali chlorides evaluated for a polarizable and non-polarizable model. *J Chem Phys*. 2020;153(1):011101. doi:10.1063/5.0012253

84. Liptak MD, Shields GC. Experimentation with different thermodynamic cycles used for pKa calculations on carboxylic acids using complete basis set and Gaussian-n models combined with CPCM continuum solvation methods. *Int J Quantum Chem*. 2001;85(6):727-741. doi:10.1002/qua.1703

85. Aragones JL, Sanz E, Valeriani C, Vega C. Calculation of the melting point of alkali halides by means of computer simulations. *J Chem Phys*. 2012;137(10):104507. doi:10.1063/1.4745205

86. Walz M-M, van der Spoel D. Systematically improved melting point prediction: a detailed physical simulation model is required. *Chem Commun*. 2019;55(80):12044-12047. doi:10.1039/C9CC06177K

87. Ladd MFC, Lee WH. The solubilities of some inorganic halides. *Trans Faraday Soc*. 1958;54:34. doi:10.1039/tf9585400034

88. Kaya S, DeFarias RF. Lattice energies from hydration enthalpies: some acid-base and structural considerations. *Int J Adv Eng Res Sci*. 2018;5(8):317-323. doi:10.22161/ijaers.5.8.39

89. Tissandier MD, Cowen KA, Feng WY, et al. The proton's absolute aqueous enthalpy and Gibbs free energy of solvation from cluster-ion solvation data. *J Phys Chem A*. 1998;102(40):7787-7794. doi:10.1021/jp982638r

90. Rueda Espinosa KJ, Kananenka AA, Rusakov AA. Novel computational chemistry infrastructure for simulating astatide in water: from basis sets to force fields using particle swarm optimization. *J Chem Theory Comput*. 2023;19(22):7998-8012. doi:10.1021/acs.jctc.3c00826

91. Rodríguez-Segundo R, Gijón A, Prosmiti R. Quantum molecular simulations of micro-hydrated halogen anions. *Phys Chem Chem Phys*. 2022;24(24):14964-14974. doi:10.1039/D2CP01396G

92. Chamorro Y, Flórez E, Maldonado A, Aucar G, Restrepo A. Microsolvation of heavy halides. *Int J Quant Chem*. 2021;121(7):e26571. doi:10.1002/qua.26571

93. Cordero B, Gómez V, Platero-Prats AE, et al. Covalent radii revisited. *Dalton Trans*. 2008;(21):2832-2838. doi:10.1039/b801115j

94. Chang Z, Li J, Dong C. Ionization potentials, electron affinities, resonance excitation energies, oscillator strengths, and ionic radii of element Uus (Z = 117) and astatine. *J Phys Chem A*. 2010;114(51):13388-13394. doi:10.1021/jp107411s

95. Haynes W. *CRC handbook of chemistry and physics*. 95th ed; 2014.

96. Gujt J, Bešter-Rogač M, Hribar-Lee B. An investigation of ion-pairing of alkali metal halides in aqueous solutions using the electrical conductivity and the Monte Carlo computer simulation methods. *J Mol Liq*. 2014;190:34-41. doi:10.1016/j.molliq.2013.09.025

SUPPORTING INFORMATION

Additional supporting information can be found online in the Supporting Information section at the end of this article.